THE JOURNAL OF PHYSICAL CHEMISTRY C
A JOURNAL OF THE AMERICAN CHEMICAL SOCIETY

pubs.acs.org/JPCC
Article

Uncovering the Screening-Enhanced Behavior of Poly(hexamethylene biguanide) Hydrochloride in Overcoming Charge Screening Limitations

Chun Yang, Wenyi Wang,* Peng Liu, Peng Tao, Haijie Cao, Ka-Fu Yung,* and Chi-Wai Kan*

Cite This: J. Phys. Chem. C 2025, 129, 2691−2700

Read Online

ACCESS | Metrics & More | Article Recommendations | Supporting Information

ABSTRACT: Conventional ionic polymers can effectively adsorb small molecules of opposite charges, but their applications are limited by the consensus that inorganic salt ions typically screen electrostatic binding between them. This weakness results in significant deterioration in the performance of electrostatic-dominant chemical processes. Herein, we reported that cationic poly(hexamethylene biguanide) (PHMB) exhibits an exceptional screening-enhanced effect, enabling its flocculation performance to be enhanced by salt ions rather than weakened by them. Flocculation experiments and theoretical simulations revealed that the superior performance of PHMB is attributed to its abundant biguanide groups, enabling screening-enhanced behavior through stable PHMB-dye adsorption, increased same-segment stacking, and a moderately enhanced hydrophobic effect in high-salt environments. This study may lay a solid foundation for developing screening-enhanced materials with the powerful capabilities of overcoming charge screening limitations for specific application scenarios.

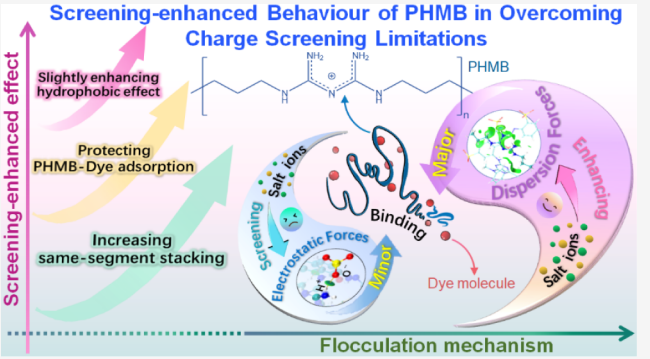

1. INTRODUCTION

The charge screening effect (i.e., Debye screening), caused by the presence of inorganic salts, is a ubiquitous phenomenon in nature.[1−3] It weakens the zeta potential of large molecules in aqueous solution and thus inevitably exerts a negative influence on the system. For example, it can severely cripple the sensitivity of electronic biosensors and compromise the flocculation performance of cationic polymeric coagulants/flocculants in both microalgae harvesting and dyeing wastewater treatment, leading to increased flocculant dosage and elevated cost.[4−6] Therefore, there is a great need to develop highly efficient screening-enhanced materials to address charge screening limitations. Inspired by the model of van de Steeg et al., who scrutinized the charge screening effects by theoretical calculations and predicted the existence of a screening-enhanced effect,[7] we firmly believe that there must exist some screening-enhanced materials that are capable of effectively overcoming charge screening limitations.

Poly(hexamethylene biguanide) (PHMB), one of the major biguanide-containing polymeric derivatives, could be an answer. Due to the unique molecular structural properties such as the rigid active biguanide moieties and flexible alkyl linking groups, PHMB exhibits self-folding behavior enthalpically driven by the like-charge pairing of the biguanide units (Figure 1a), making the adsorption reaction a fast kinetic process.[8] The significant HOMO−LUMO energy gap of PHMB also favors its stable chemical skeleton and thermal stability.[9] Additionally, the biguanide group has three tautomeric resonance forms, which implies that biguanide-bearing cationic polyelectrolytes such as PHMB have high proton mobility and pH-tolerant properties owing to the delocalization of charges.[10−12] We substantiated that PHMB possesses remarkable flocculation performance and can effectively overcome charge screening limitations, thereby greatly reducing the dosages and cost of wastewater treatment (Figure 1b).[13] The color removal efficiency could reach up to 91.5% with the PHMB dosage as low as 40 mg·L^{-1} by increasing the concentration of NaCl to 200 mmol·L^{-1}. This reflects the increased flocculation degree of PHMB targeting dye molecules with increasing ionic strength.

However, the mechanism of action of the screening-enhanced effect is unclear. Blackburn et al. observed that the stacking of PHMB trimers became more favorable in the presence of chloride ions.[14] Studies on the self-assembly of PHMB and similar polyelectrolytes suggested that the

Received: October 17, 2024
Revised: January 15, 2025
Accepted: January 16, 2025
Published: January 29, 2025

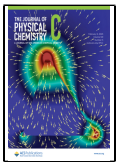

https://doi.org/10.1021/acs.jpcc.4c07047
J. Phys. Chem. C 2025, 129, 2691−2700

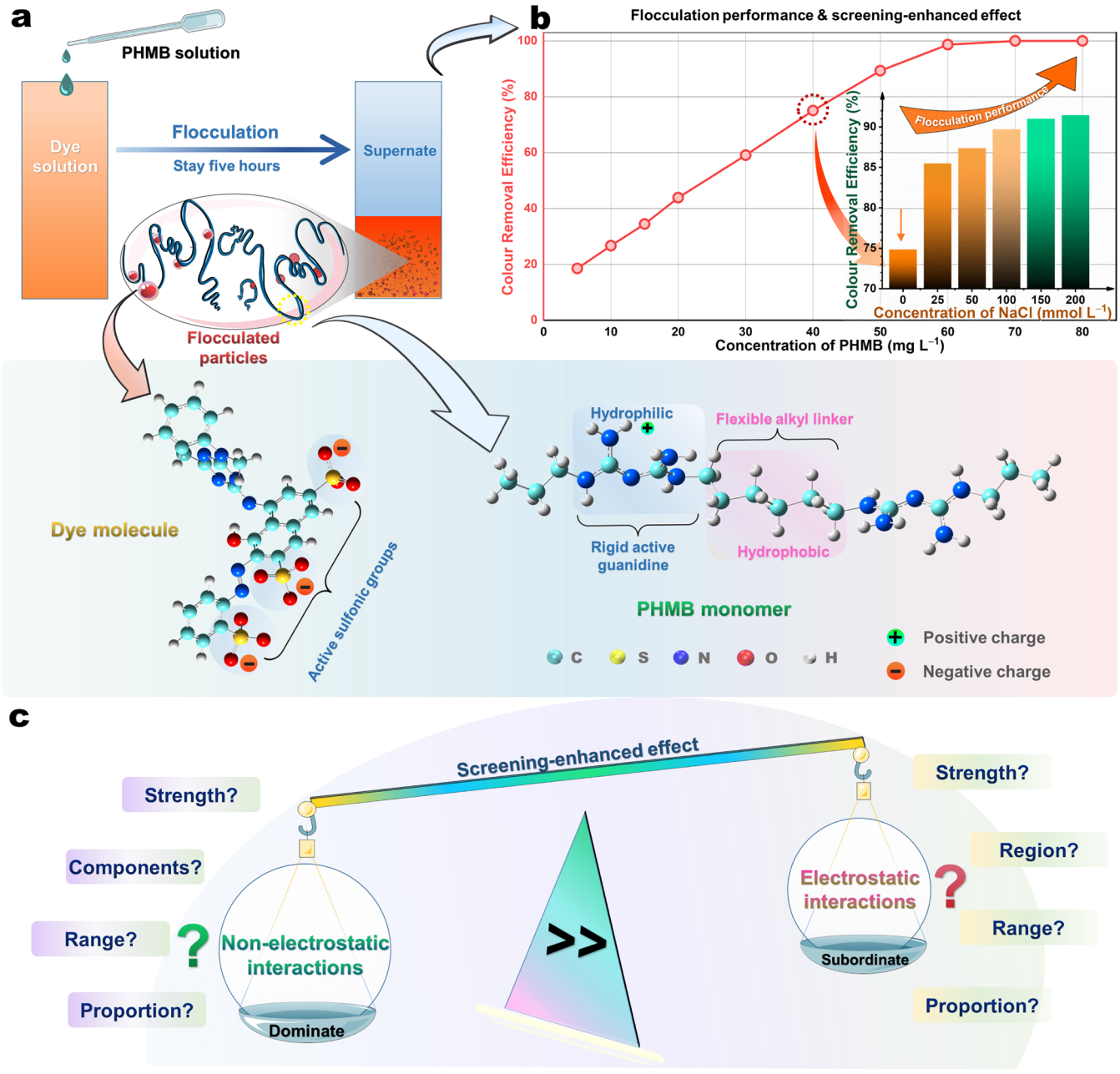

Figure 1. Flocculation performance of PHMB and the screening-enhanced effect. (a) Schematic diagram of the flocculation process. (b) Curves of decoloration efficiency with varying PHMB concentrations for the red dye (C.I. Reactive Red 24) solution. The color removal efficiency gradually reached 91.5% by progressively elevating the salt concentration when maintaining a low PHMB concentration of 40 mg·L^{-1} (inset). Below the plots are models of the red dye molecule (with one Cl atom omitted) and the PHMB monomer. (c) Based on the previous literature, we postulated that nonelectrostatic interactions, which are significantly more pronounced than electrostatic interactions, would dominate the flocculation process.

counterion condensation caused by increased ionic strength could significantly promote the adsorption interactions of PHMB-contained systems.[8,15−18] But the impact of inorganic salts on the homogeneous adsorption reactions of PHMB toward dye-like molecules remains elusive. According to the study of van de Steeg and coworkers,[7] if the electrostatic attraction was less than the nonelectrostatic force, inorganic salts would facilitate the adsorption of organic polyelectrolytes onto the solid surface, a phenomenon referred to as the screening-enhanced effect (Figure 1c). Nonetheless, this computational model considers adsorbate behavior only on a two-dimensional surface and employs a mean-field approximation, with research parameters for weak interactions based on an estimated Flory−Huggins constant lacking further in-depth exploration. Additionally, no studies have specified the actual strength, components, or distribution of nonelectrostatic forces in real chemical systems, nor their relative contribution to the overall interaction. Therefore, we conducted an in-depth study of the flocculation performance of PHMB toward anionic dye molecules in saline solutions. Our findings confirm that the essence of the nonelectrostatic interactions counteracting the electrostatic screening arises from a synthesis of various weak interactions, primarily dominated by the dispersion force. Additionally, we assessed the influence of salt ions on all interactions and their relative contribution to the screening-enhanced mechanism.

https://doi.org/10.1021/acs.jpcc.4c07047
J. Phys. Chem. C 2025, 129, 2691−2700

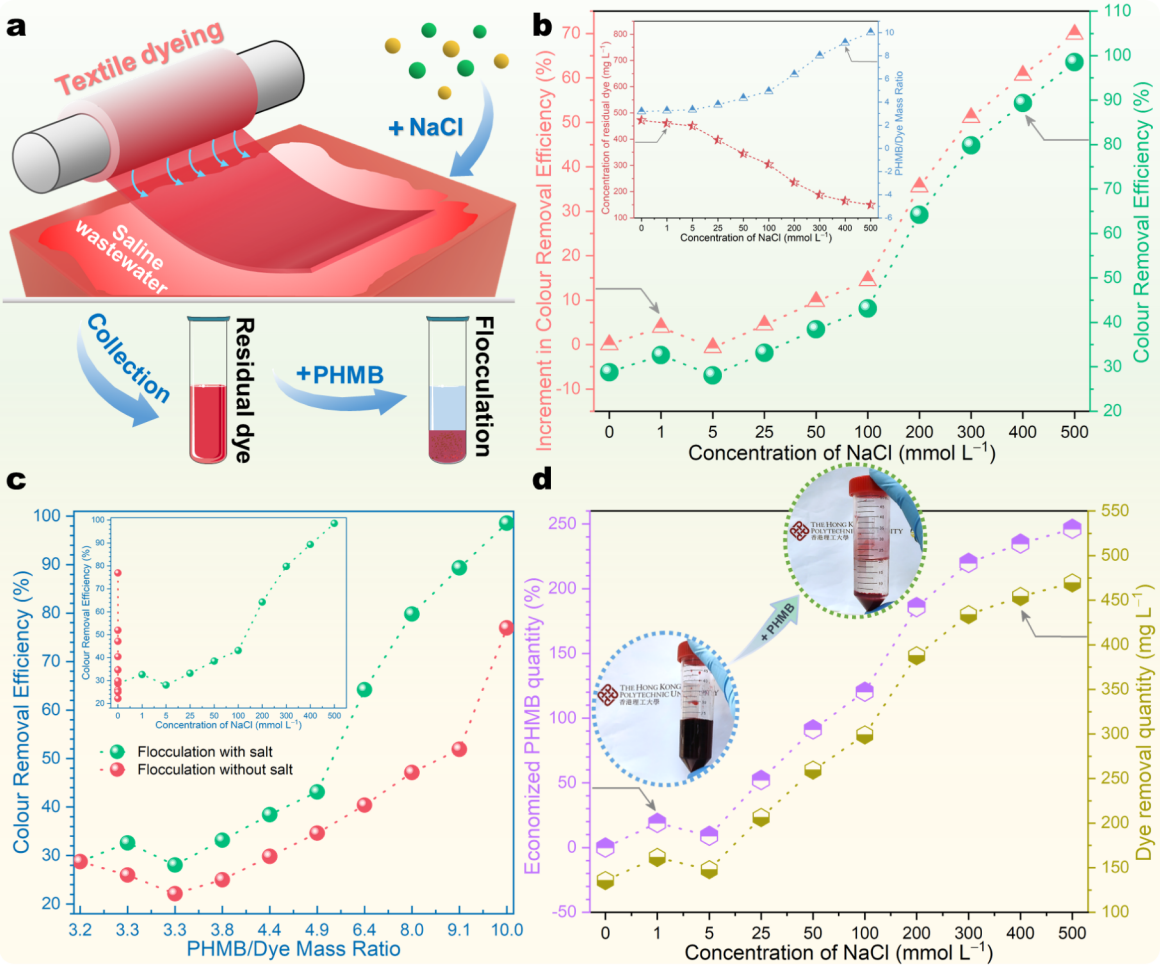

Figure 2. (a) The flocculation performance of PHMB in real dye wastewater at different salt concentrations was investigated. The dye wastewater collected after the normal dyeing of fabric with C.I. Direct Red 81 contained varying proportions of NaCl added during the dyeing process to enhance the dyeing behavior. The samples were diluted to half of the original concentrations for flocculation testing, and the concentrations of PHMB were maintained at 50 mg·L^{-1} throughout the experiment. (b) The increment in color removal efficiency varied with the salt concentration (red points), obtained from the curve of color removal efficiency (green points). The variation in dye removal quantity and PHMB/dye mass ratio in real wastewater with changing salt concentration is also exhibited in the inset. (c) To compare with the performance without added salt ions, the color removal efficiency was retested while maintaining the corresponding ratio of PHMB to dye (blue points). (d) The economized quantity of PHMB varied with increased salt concentration (purple points), derived from the curve representing the residual dye removal quantity variation under different salt concentrations (yellow points). The photos depicted the before-and-after states of flocculation in wastewater containing 500 mmol·L^{-1} NaCl (with 200 mg·L^{-1} of PHMB).

2. EXPERIMENTAL METHODS

2.1. Flocculation Experiments of PHMB. To measure the flocculation ability of PHMB for the dye-containing wastewater, PHMB solutions in the concentrations of 5, 10, 15, 20, 30, 40, 50, 60, 70, and 80 mg·L^{-1} were prepared and the concentration of dye was kept at 100 mg·L^{-1}. The mixtures were left to stand undisturbed for 5 h before further testing. The turbidity values and zeta potentials were measured by assaying the supernatant, which was filtered through a 0.45-μm filter before absorbance measurements. The concentration of the dye solution after flocculation was determined by using a premeasured standard curve, and the color removal efficiency was subsequently calculated based on Eq S1. To examine the influence of a high-salt environment on the flocculation efficacy of PHMB, varying quantities of NaCl crystals were preintroduced to achieve the final NaCl concentrations of 1, 5, 25, 50, 100, 150, 200, 250, 300, 400, and 500 mmol·L^{-1}. Details of the experiments and the calculation methods for flocculation performance can be found in Part 1 (Flocculation experiments of PHMB) and Part 2 (Screening-enhanced effect of PHMB in real dyeing wastewater) of the Supporting Information.

2.2. Computational Methods. For DFT simulations, preliminary optimized structures were generated using Gaussian16 software with the B3LYP-GD3BJ functional and the DFT-D3 method employing Becke-Johnson damping for weak interaction corrections. The TZVP basis sets were employed to ensure adequate accuracy at this stage. For a more precise analysis of noncovalent interactions involving main group elements, the M06-2X density functional and multifuse def2-TZVP basis sets with dispersion correction were employed for single-point energy calculations. These simulations also incorporated the SMD (solvation model based on density) explicit solvent model to account for solvent effects. Preparatory work for the simulations, such as determining the lowest energy configurations, as well as the subsequent DFT analysis methods, is detailed in Part 3 (DFT computational methods) of the Supporting Information. Additionally,

https://doi.org/10.1021/acs.jpcc.4c07047
J. Phys. Chem. C 2025, 129, 2691−2700

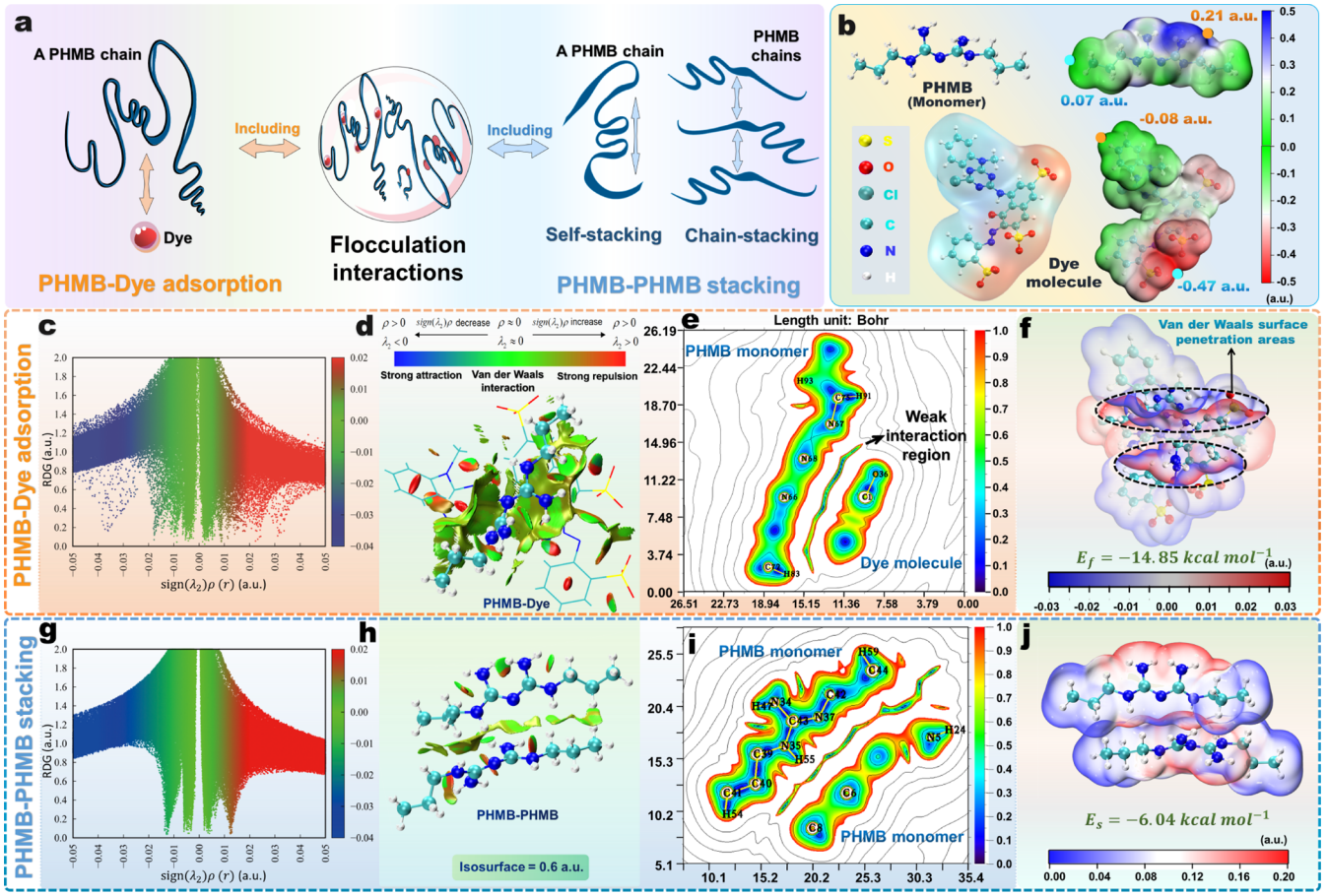

Figure 3. (a) Schematic diagram illustrating the flocculation forces, showing PHMB-dye adsorption as well as PHMB−PHMB stacking; (b) the van der Waals surfaces of the PHMB monomer and the dye molecule. The yellow and blue dots represent the maximum and minimum ESP points, respectively; (c,g) the RDG-$sign(\lambda_2)\rho(r)$ scatter diagrams of the PHMB-dye adsorption and PHMB−PHMB stacking systems; (d,h) a local image of RDG isosurfaces (0.6 au) reflecting weak intermolecular interaction areas in the PHMB-dye complex or PHMB−PHMB stacking structure, the top of which is the interpretation of coloring method of mapped function $sign(\lambda_2)\rho(r)$; (e,i) a plot of a color-filled map of RDG in the plane determined by three atoms (C1 atom of the dye molecule, N66 atom of the PHMB monomer, and N67 atom of PHMB the monomer) for the PHMB-dye complex and the RDG sectional drawing for the PHMB−PHMB stacking system; (f,j) the corresponding van der Waals penetration diagrams of PHMB-dye adsorption and PHMB−PHMB stacking adsorption systems. E_f is the energy barrier value for forming the PHMB-dye complex, and E_s is the energy barrier value for forming the stacked structure of PHMB monomers (M06-2X/ma-def2-TZVP). All results were obtained from Gaussian16 software and Multiwfn program and visualized using VMD (visual molecular dynamics) software.[19−21] The van der Waals penetration graphs and the RDG graphs in the 3D animation were uploaded to the Figshare website (10.6084/m9.figshare.23937087).

molecular dynamics simulation was also performed at 298.15 K in the NPT ensemble for 1000 ns by GROMACS/2023 software based on the GAFF force field parameters produced from the Sobtop program and the RESP (restrained electrostatic potential) charge generated by the Multiwfn program. Details of the parameter settings can be found in Part 4 (Molecular dynamics simulation) of the Supporting Information.

3. RESULTS AND DISCUSSION

In order to better understand the screening-enhanced behavior, we first repeated the flocculation experiments of PHMB on various anionic dyes, and the results demonstrate that PHMB is highly salt tolerant and is able to effectively surmount the charge screening limitations (Figure S1). We also employed the real dyeing wastewater containing a great amount of inorganic salts to investigate this effect. As shown in Figure 2a, unlike the common cationic polymeric flocculants, the screening-enhanced effect can make PHMB effectively avoid performance degradation in salty environments. An increase in the concentration of salt added in the dyeing process significantly reduced the residual dye concentration while maintaining an enhanced dyeing rate and dye uptake (Figure 2b (inset)). The increment in color removal efficiency (eq S2) resulting from increasing NaCl concentration could reach 69.8% at 500 mmol·L^{-1} NaCl compared to that without salts (Figure 2b). If the mass ratio of PHMB to the residual dye was maintained, the flocculation activities of PHMB in the presence of salt ions always outperformed the counterparts without salts (Figure 2c), indicating that the color removal efficiency in salt-containing wastewater was significantly improved due to the screening-enhanced effect. Moreover, an economized quantity of PHMB (eq S3) exhibited a remarkable improvement, being up to 246.2% at 500 mmol·L^{-1} NaCl in comparison to the salt-free wastewater environment (Figure 2d).

Based on the characteristics of flocculation interactions, they can be divided into two parts: the interactions between PHMB and dye molecules and the stacking interactions among PHMB molecules themselves (Figure 3a). The van der Waals surface

https://doi.org/10.1021/acs.jpcc.4c07047
J. Phys. Chem. C 2025, 129, 2691−2700

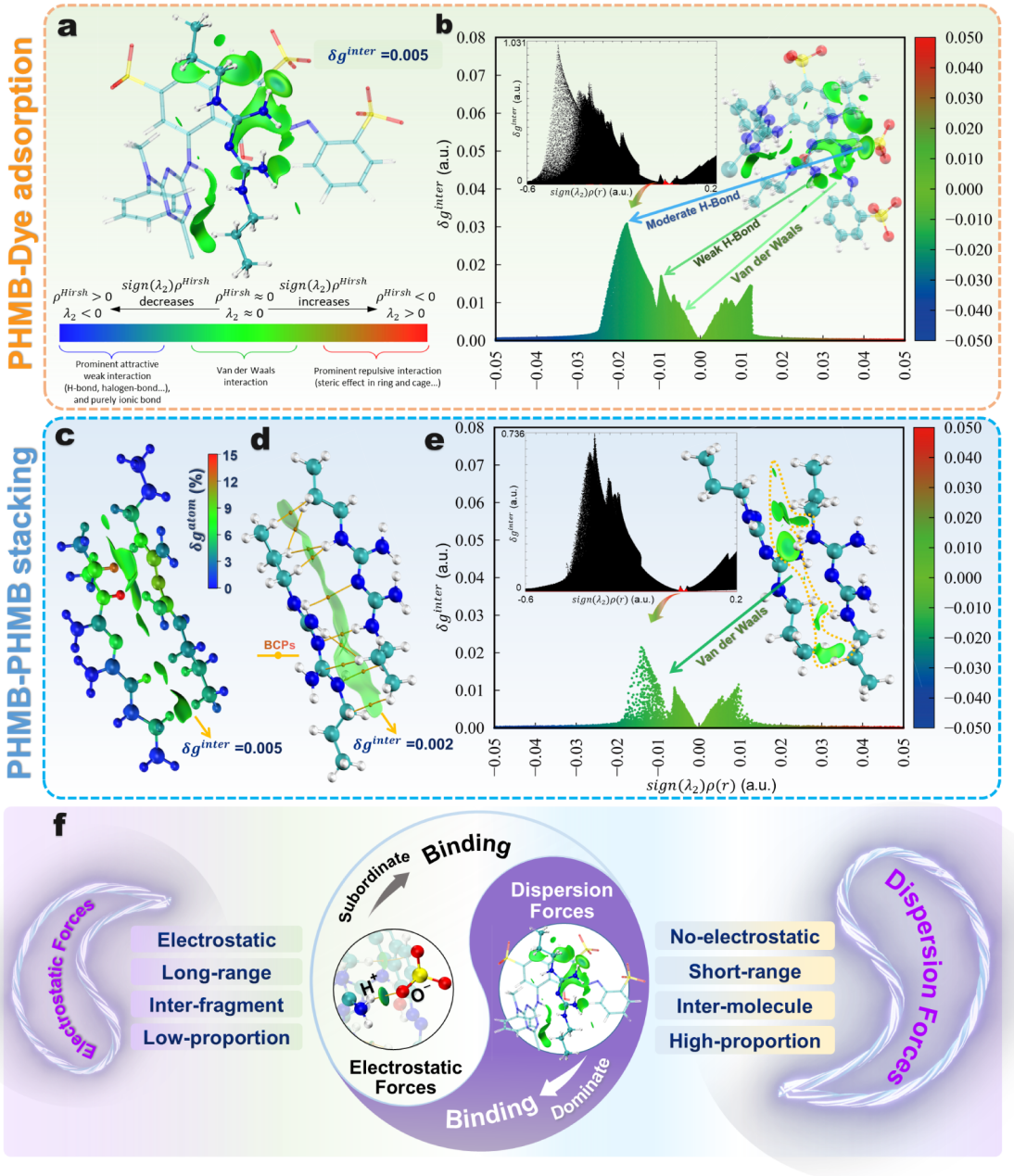

Figure 4. (a,c) Isosurfaces of δg^{inter} at 0.005 au colored by $sign(\lambda_2)\rho^{\text{Hirsh}}(r)$, and each molecule is defined as a fragment in the PHMB-dye adsorption or PHMB−PHMB stacking systems, below which is the coloring method of the $sign(\lambda_2)\rho^{\text{Hirsh}}(r)$ function; (b,e) the corresponding IGMH scatter plot of PHMB-dye and PHMB−PHMB stacking systems with an abscissa range of (−0.6, 0.2) is also shown (inset), in which a red region highlighting weak interaction areas further magnified in the color-filled diagram with an abscissa range of (−0.05, 0.05) below. The small positive peaks on the right side of the plot indicate the presence of relatively minor steric hindrance in the system; (d) reducing the δg^{inter} isosurface to 0.002 au; main BCPs (bond critical points) are visible. Main BCPs with brown bond path lines are marked by red arrows (right); (c−e) The corresponding δg^{atom} percentages (c), BCPs (d) and IGMH analyses (e) in the PHMB−PHMB stacking adsorption system. (f) the proposed weak-interaction-dependent mechanism for the flocculation action of PHMB. The IGMH graphs in the 3D animation was uploaded to the Figshare website (10.6084/m9.figshare.23937114).

of each molecule shows the active site −NH−H$^+$ of the biguanide group in the PHMB molecule and the active $-SO_3^-$ group of the dye molecule, respectively (Figure 3b). However, there is no formation of strong electrostatic bonds between these two polar molecules; instead, they are bound together by weak interactions as reduced density gradient (RDG)[22] analysis according to eqS8 shown in Figure 3c−e. For the PHMB-dye complex, the large areas of green-colored isosurfaces display the presence of intermolecular weak interactions between the PHMB monomer and the dye molecule. Various van der Waals interpenetrating regions between both molecules further prove the apparent existence of weak interactions in their complex (Figure 3f). Moreover, the mutual penetration between the biguanide and a sulfonic acid group is approximately 2 nm (Figure S7), indicative of a significantly weak interaction between active sites. The energy barrier value for the flocculation reaction (E_b, as defined in eqs S4−S7) is −14.85 kcal·mol^{-1}, which also reflects the pronounced binding affinity of PHMB to the dye molecule.

https://doi.org/10.1021/acs.jpcc.4c07047
J. Phys. Chem. C 2025, 129, 2691−2700

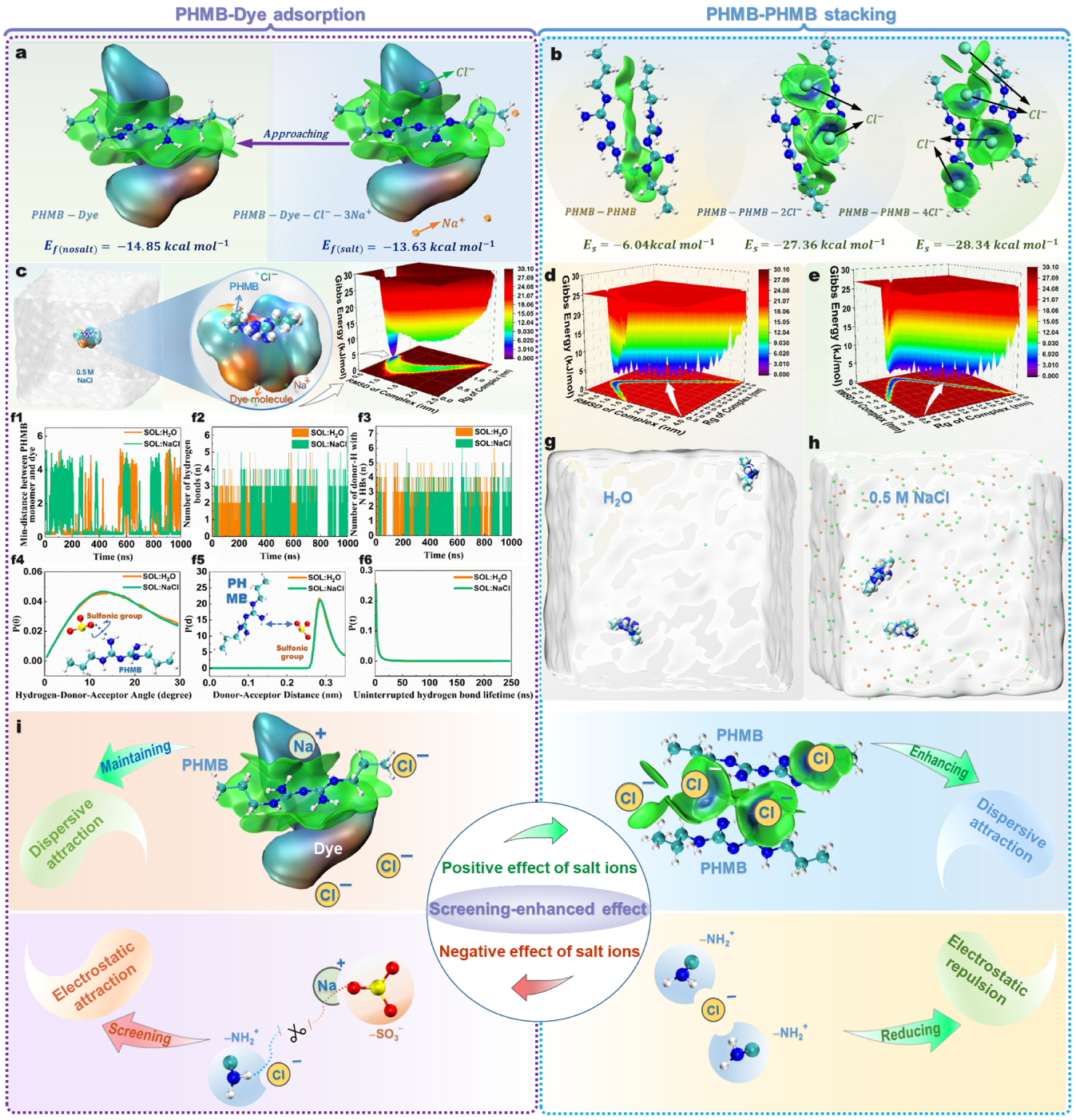

Figure 5. In the flocculation model within NaCl saline solution, various interactions can be divided into intermolecular interactions (a,c,f,i(left)) and same-segment interactions (b,d,e,g,h,i(right)): (a) by calculating the ground-state energy difference between PHMB(Cl^-)-dye($3Na^+$) and the sum of PHMB(Cl^-) and dye($3Na^+$), the energy barrier of flocculation in the presence of inorganic salt ions, denoted as $E_{f(salt)}$, can be determined. $E_{f(no\ salt)}$ is the energy barrier of flocculation in the absence of inorganic salt ions. The isosurface of δg^{inter} at 0.001 au is visualized to examine the variations in weak interactions between PHMB and dye; (b) the energy differences between different PHMB−PHMB stacking systems with different Cl^- ion ratios. The isosurfaces of δg^{inter} at 0.001 au among three fragments (the chloride ion acts as one fragment, while each PHMB monomer serve as a fragment) are also presented; (c) in the model system for the PHMB-dye complex in 0.5 M NaCl solution, the configuration extracted from one frame (frame number 499141: about 998 ns) with the lowest Gibbs energy during the dynamic process in 0.5 M NaCl solution and the corresponding free energy landscape (FEL) are illustrated, in which RMSD and R_g of the PHMB-dye complex were the X value and Y value, respectively. The movies of 1000 ns formal dynamics simulation for the PHMB-dye complex in 0.5 M NaCl or water solution were uploaded to the Figshare website (10.6084/m9.figshare.23936832). Comparison of Min-distance (f1), HBs (the number of hydrogen bonds) (f2), and the number of donor-H with N HBs (f3) between the PHMB monomer and dye molecule in water and NaCl solution. Comparison of the donor−acceptor angle (f4), donor−acceptor distance (f5), and uninterrupted lifetime (f6) for donor-H with N HBs in water and NaCl solution. In the PHMB−PHMB stacking systems, frames corresponding to the lowest point in FEL graphs in water solution (d,g) and 0.5 M NaCl solution (e,h) are exhibited individually.

https://doi.org/10.1021/acs.jpcc.4c07047
J. Phys. Chem. C 2025, 129, 2691−2700

What is even more remarkable is that even without anions neutralizing the charges in the PHMB stacking system, no repulsion occurs between the two positively charged PHMB monomers. They can still interact and bind through similar weak interactions as RDG plots shown in Figure 3g−i). Moreover, ESP penetration maps indicate the formation of stable stack structures between PHMB segments (Figure 3j). For the PHMB−PHMB system, the energy barrier value of stacking adsorption (E_s) remains considerable (−6.04 kcal·mol^{-1}). This may explain why PHMB exhibits excellent flocculation performance because the chemical adsorption occurs not only between PHMB and dye molecules but also between PHMB segments.

Subsequently, we explored the properties and characteristics of these weak interactions, especially the strength, bonding forms, range, and relative contribution of nonelectrostatic components to the total weak interactions. According to the independent gradient model based on Hirshfeld partition (IGMH)[23] analysis, the extensive green-color isosurface (δg^{inter} = 0.005, defined as eqs S9 and S10) suggests that there were various weak interactions in the PHMB-dye adsorption system (Figures 4a and S10). These weak interactions can be assigned to moderate-strength hydrogen bonds (H-bond), weak-strength H-bonds, and intermolecular van der Waals forces (Figure 4b).[24,25] Then, we evaluated the contributions of atomic pairs and atoms to total forces (δg^{pair} and δg^{atom}) according to eqs S11-S16. The specific H-bonds of N−H···O, C−H···C, C−H···S, N−H···S, C−H···N, and C−H···Cl were the major contributors (>0.8%) to the total interactions (Figure S12). Among them, the H-bond between the polar active sites (N−H···O) had the highest atomic pair contribution (δg^{pair}= 2.12%) and the highest electron density at a certain bond critical point ($\delta\rho_{BCP}$ = 0.03 au) (Figure S13). The other $\delta\rho_{BCP}$ values can be found in the Supporting Information IGMH.zip. Both weak hydrogen bonds and intermolecular van der Waals forces are weaker than the moderate-strength N−H···O hydrogen bond, but all are dominated by dispersion forces arising from polarization fluctuations between neighboring particles. Figures 4c−e, S11 and S14 further illustrate that similar dispersion-dominated weak interactions were also abundant in the PHMB−PHMB stacking adsorption system, which resulted in the mutual attraction and stacking between PHMB chain segments. All of the above H-bonds and van der Waals forces are dispersion-dominated weak interactions, establishing a vast weak-binding network through flexible intermolecular contact. Meanwhile, the weak interactions can accumulate owing to numerous repeating units of the long-chain PHMB macromolecule, thereby enhancing the adsorption capacity toward dye molecules. Hence, as predicted by the model of van de Steeg, the nonelectrostatic, high-proportion, short-range intermolecular dispersion forces in the system far exceed the low-proportion, long-range interfragment electrostatic forces, enabling PHMB to achieve highly efficient flocculation via the nonelectrostatic interactions (Figure 4f).

The strong and extensive nonelectrostatic dispersion attractions between PHMB and small molecules, as well as among PHMB chain segments, mainly arise from the unique electronic delocalization structure of PHMB. According to the anisotropy of the induced current density (AICD) map of a PHMB monomer (Figure S15),[26] it was found that the valence electrons within the biguanide backbone were effectively delocalized, which provides an explanation for the stable adsorption with dye molecules and effective stacking between positively charged PHMB chain segments. Analysis of the orbital interactions through the extended transition state-natural orbitals for chemical valence (ETS-NOCV)[27] method further reveals the electron transfer occurring in both the PHMB-dye and PHMB-stacking structures. As shown in Figure S16a, the NOCV pair 1 of the PHMB-dye complex had the largest energy (−4.89 kcal·mol^{-1}), with an eigenvalue of 0.17, accounting for the main part of the total orbital interactions. Further analysis reveals that it corresponded to the moderate H-bond (N−H···O) interaction. This orbital interaction led to a region with an increased electron density between the hydrogen atom of biguanide in PHMB and the oxygen atom of the $-SO_3^-$ group in the dye molecule (as the hydrogen bond receptor), indicative of the feature of a moderate-strength hydrogen bond. More interestingly, the −NH−, $-NH_2-$ or adjacent $-CH_2-$ groups had orbital interactions with the benzene ring of the dye molecule. Especially for NOCV pair 2, the delocalized electrons on the biguanides were even conjugated with π electrons of the benzene ring. It was also found that electron transfer occurs between two PHMB monomers due to active delocalized electrons within the biguanide backbone, facilitating efficient stacking between positively charged PHMB chain segments (Figure S16b). Hence, the properties of PHMB impart the biguanide compound with pronounced reactivity and facilitate strong interactions with surrounding molecules or PHMB segments. All the NOCV pairs can be found in the corresponding Supporting Information (NOCV.zip). HOMO−LUMO orbital diagrams (Figure S17) also demonstrate that the biguanide groups not only facilitate the formation of hydrogen bonds through primary active sites but also interact with the orbit of the dye molecular heterocyclic rings, leading to the formation of a stable complex.

Surprisingly, the energy barrier of flocculation in the presence of inorganic ions ($E_{f(salt)}$ = −13.63 kcal·mol^{-1}) was slightly greater than that without inorganic salts ($E_{f(nosalt)}$ = −14.85 kcal·mol^{-1}) (Figure 5a). The difference between them is insignificant, suggesting that the influence of inorganic ions on the adsorption mode between PHMB and the dye molecules was negligible. The distinct green IGMH isosurfaces further indicate that the weak interactions between PHMB and the dye were hardly influenced by the presence of Na^+ and Cl^- ions (Figure 5a). According to the molecular dynamics simulation (GROMACS/2023 software using the GAFF force field),[28−30] the frames associated with the lowest Gibbs energy in 0.5 M NaCl solution (Figure 5c) exhibited a similar binding structure to that in D.I. water solution in Figure S19, which indicates the resistance of intermolecular binding forces to electrostatic shielding. In the presence of salt ions, PHMB can still form a stable complex with the dye molecule (Figures S20 and S21). The minimum adsorption distance (Figure 5f1) and the number of hydrogen bonds (Figure 5f2,f3) between PHMB and the dye molecule were hardly affected by the presence of NaCl solute. The almost identical hydrogen bond angles, donor−acceptor distances, and uninterrupted hydrogen bond lifetimes of the N−H···O H-bond in both NaCl and aqueous solution (Figure 5f4−f6) also prove that the influence of salt ions on PHMB-dye adsorption was not significant.

Furthermore, the PHMB−PHMB stacking adsorption was enhanced by the increased chloride ions, as shown in Figure 5b. The PHMB segments could always attract each other via van der Waals forces (Figure S18), irrespective of the number

https://doi.org/10.1021/acs.jpcc.4c07047
J. Phys. Chem. C 2025, 129, 2691−2700

of chloride ions (0, 2, or 4). Additionally, as depicted in the IGMH isosurfaces in Figure 5b, each chloride ion was encircled by a green floral-shaped isosurface, which reveals the existence of a weak interaction. Chloride ions acted as'adhesive' agents, generating electrostatic attractions and van der Waals interactions between PHMB segments and the inorganic ions, thereby enhancing the stability of PHMB−PHMB stacking. A shorter distance between PHMB segments in the frame (corresponding to the lowest point in the free energy landscape (FEL)) in NaCl solution in Figure 5e,h than that in pure water solution in Figure 5d,g also verified the enhanced same-segment adsorption. This is consistent with the results obtained by using the OPLS-AA force field to simulate the self-assembly behavior of PHMB.[8]

Both the energy decomposition analysis for the weak interaction energies method (sobEDAw)[31] and molecular mechanics/Poisson−Boltzmann surface area calculations (MM/PBSA)[32,33] further clarify the impact of salt ions on various weak interactions. The results in Tables S1 and S2 confirm that salt ions only shielded the electrostatic attraction, which contributed minimally to the total binding forces and hardly changed the essential dispersion interactions for PHMB-dye adsorption. By contrast, the salt ions significantly reduced the same-segment electrostatic repulsion and enhanced the dispersion forces and orbital interactions between PHMB segments, which can also be indirectly supported by variation curves of Coul-SR and LJ-SR in Figure S22 and interrelated values in Table S3. Notably, as shown in Figure S21, the hydrophobic surface areas of the PHMB-dye complex were greater than the hydrophilic areas. MM/PBSA calculations also showed that the ΔE_{solv} of the complex system was 5.03 kcal/mol lower in the simulated solution of 0.5 M NaCl (145.51 kcal/mol) than in water (150.54 kcal/mol) (Table S2), reflecting the hydrophobic effect of the complex system. The nonelectrostatic terms (ΔCDS, Equation S17 after Table S1) in the sobEDAw analysis also indirectly reflect a tiny trend of the hydrophobic effect driving the formation of the PHMB-dye or PHMB−PHMB complex.[34,35] However, the contribution of hydrophobic effects to the screening-enhanced behavior is minimal and not sensitive to ionic strength;[36] the primary factors are the stable PHMB-dye adsorption and the enhanced PHMB−PHMB stacking.

Thus, the screening-enhanced effect of PHMB is well explained by the combination of steady PHMB-dye adsorption, increased same-segment stacking, and a slightly enhanced hydrophobic effect, which collectively enhance flocculation activity, leading to an elevated color removal efficiency of up to 100% at high concentrations of salt ions. This aligns with the screening-enhanced weak-interaction-dependent mechanism illustrated in Figure 5i, primarily governed by dispersion forces, which counteract the screening effect of inorganic salt ions, thereby preventing the attenuation of the binding interactions during the flocculation process in a highly saline environment.

4. CONCLUSION

In conclusion, the present work thoroughly studied the screening-enhanced effect of PHMB by using theoretical calculations based on DFT and wave function analysis. It was found that the adsorption between PHMB and dye molecules primarily relies on the moderate-strength hydrogen bond, weak-strength hydrogen bonds, and notable intermolecular van der Waals forces, indicating a weak-interaction-dependent mechanism. The biguanide groups of PHMB serve as the primary active adsorption sites for flocculation and activate the hydrogen atom activity in neighboring alkyl chains, which raises the possibility of binding for the flocculation process. Through molecular dynamics simulations, the underlying mechanism for overcoming the charge shielding effect was elucidated. Salt electrolyte ions hardly affect the weak interactions that maintain intermolecular adsorption but increase PHMB intersegment stacking absorption and slightly promote the hydrophobic effect of flocculation complexes. As a result, as the salt concentration increases, this mechanism not only preserves the steady PHMB-dye adsorption and enhances same-segment stacking but also strengthens the hydrophobic effect, which triggers the screening-enhanced effect and facilitates flocculation performance. This contributes positively to the flocculation process in high-salt environments, resulting in an improvement in color removal efficiency at low PHMB concentrations. For the real dyeing wastewater treatment, the flocculation performance can be enhanced by 69.8% at a higher salt concentration, and the cost can be decreased by 246.2%. Therefore, the screening-enhanced effect makes PHMB a highly promising candidate for real saline colored wastewater treatment. Meanwhile, the present study may also facilitate a better understanding toward the anticharge screening effect and inspire more researchers to develop innovative screening-enhanced polymeric materials to surmount the charge screening limitations in practical applications.

■ ASSOCIATED CONTENT

Supporting Information

The Supporting Information is available free of charge at https://pubs.acs.org/doi/10.1021/acs.jpcc.4c07047.

Flocculation experiments with PHMB, the screening-enhanced effect of PHMB in real dyeing wastewater, DFT computations, and molecular dynamics simulation methods (PDF)

MD.zip Input files for GROMACS/2023 software (initial structure, molecular topology, and all simulation parameters) for dynamics simulation of the PHMB-dye and PHMB-PHMB systems in 0.5 M NaCl or water solution. NOCV.zip All NOCV pairs in the PHMB-dye adsorption and PHMB-PHMB stacking systems. IGMH.zip The IGMH analysis output results (including each atom's structure, contribution to the total forces, related bond critical points, etc.) (ZIP)

■ AUTHOR INFORMATION

Corresponding Authors

Wenyi Wang − *Department of Applied Biology and Chemical Technology, The Hong Kong Polytechnic University, Hung Hom, Hong Kong 999077, China;* orcid.org/0000-0001-6923-8613; Email: wang.wenyi@polyu.edu.hk

Ka-Fu Yung − *Department of Applied Biology and Chemical Technology, The Hong Kong Polytechnic University, Hung Hom, Hong Kong 999077, China*; Email: kf.yung@polyu.edu.hk

Chi-Wai Kan − *School of Fashion and Textiles, The Hong Kong Polytechnic University, Hung Hom, Hong Kong 999077, China;* orcid.org/0000-0002-7668-2410; Email: kan.chi.wai@polyu.edu.hk

https://doi.org/10.1021/acs.jpcc.4c07047
J. Phys. Chem. C 2025, 129, 2691−2700

Authors

Chun Yang − *Department of Applied Biology and Chemical Technology, The Hong Kong Polytechnic University, Hung Hom, Hong Kong 999077, China*

Peng Liu − *Department of Applied Biology and Chemical Technology, The Hong Kong Polytechnic University, Hung Hom, Hong Kong 999077, China*

Peng Tao − *Department of Applied Biology and Chemical Technology, The Hong Kong Polytechnic University, Hung Hom, Hong Kong 999077, China;* orcid.org/0000-0003-1932-557X

Haijie Cao − *Institute of Materials for Energy and Environment, School of Materials Science and Engineering, Qingdao University, Qingdao 266071, China*

Complete contact information is available at: https://pubs.acs.org/10.1021/acs.jpcc.4c07047

Notes

The authors declare no competing financial interest.

■ ACKNOWLEDGMENTS

We sincerely appreciate the financial support from The Hong Kong Polytechnic University (project number: A0041548) and the Innovation and Technology Commission with the funding scheme Innovation and Technology Fund-The Hong Kong Research Institute of Textiles and Apparel (ITF-HKRITA, project number: ITP/032/22TP). We also appreciate the assistance of Prof Bolong Huang from the Department of Chemistry at City University of Hong Kong in the theoretical calculation analysis.

■ REFERENCES

(1) Kornyshev, A. A. Double-Layer in Ionic Liquids: Paradigm Change? *J. Phys. Chem. B* **2007**, *111* (20), 5545−5557.

(2) Lynden-Bell, R. M.; Frolov, A. I.; Fedorov, M. V. Electrode Screening by Ionic Liquids. *Phys. Chem. Chem. Phys.* **2012**, *14* (8), 2693−2701.

(3) Park, S.-W.; DeYoung, A. D.; Dhumal, N. R.; Shim, Y.; Kim, H. J.; Jung, Y. Computer Simulation Study of Graphene Oxide Supercapacitors: Charge Screening Mechanism. *J. Phys. Chem. Lett.* **2016**, *7* (7), 1180−1186.

(4) Kesler, V.; Murmann, B.; Soh, H. T. Going beyond the Debye Length: Overcoming Charge Screening Limitations in Next-Generation Bioelectronic Sensors. *ACS Nano* **2020**, *14* (12), 16194−16201.

(5) Cai, T.; Li, H.; Yang, R.; Wang, Y.; Li, R.; Yang, H.; Li, A.; Cheng, R. Efficient Flocculation of an Anionic Dye from Aqueous Solutions Using a Cellulose-Based Flocculant. *Cellulose* **2015**, *22* (2), 1439−1449.

(6) Li, S.; Hu, T.; Xu, Y.; Wang, J.; Chu, R.; Yin, Z.; Mo, F.; Zhu, L. A Review on Flocculation as an Efficient Method to Harvest Energy Microalgae: Mechanisms, Performances, Influencing Factors and Perspectives. *Renewable Sustainable Energy Rev.* **2020**, *131*, 110005.

(7) Van de Steeg, H. G. M.; Cohen Stuart, M. A.; De Keizer, A.; Bijsterbosch, B. H. Polyelectrolyte Adsorption: A Subtle Balance of Forces. *Langmuir* **1992**, *8* (10), 2538−2546.

(8) Zaki, A. M.; Troisi, A.; Carbone, P. Unexpected Like-Charge Self-Assembly of a Biguanide-Based Antimicrobial Polyelectrolyte. *J. Phys. Chem. Lett.* **2016**, *7* (19), 3730−3735.

(9) Rodrigues, A. M.; Silva, S. Y. S.; Oliveira, M. N.; de Oliveira, G. C. A.; Novais, A. L. F.; de Paula, G. F.; Souza, D. N.; Belo, E. A.; Gester, R.; Andrade-Filho, T. Prediction of Electronic and Vibrational Properties of Poly (Hexamethylene Biguanide) Hydrochloride: A Combined Theoretical and Experimental Investigation. *J. Mol. Struct.* **2021**, *1246*, 131176.

(10) Patel, D. S.; Bharatam, P. V. Divalent N(I) Compounds with Two Lone Pairs on Nitrogen. *J. Phys. Chem. A* **2011**, *115* (26), 7645−7655.

(11) Grytsai, O.; Ronco, C.; Benhida, R. Synthetic Accesses to Biguanide Compounds. *Beilstein J. Org. Chem.* **2021**, *17* (1), 1001−1040.

(12) Britz, J.; Meyer, W. H.; Wegner, G. Poly(Alkylene Biguanides) as Proton Conductors for High-Temperature PEMFCs. *Adv. Mater.* **2010**, *22* (8), No. E72−E76.

(13) Wang, W. Y.; Chiou, J. C.; Chen, W. X.; Kan, C. W.; Lam, T. Y. C.; Hu, H. Poly(Hexamethylene Biguanide): An Efficient pH-Tolerant and Salt-Intensive Flocculant in the Removal of Anionic Dyes from Wastewater. *J. Mater. Sci.* **2022**, *57* (32), 15662−15673.

(14) Blackburn, R. S.; Harvey, A.; Kettle, L. L.; Payne, J. D.; Russell, S. J. Sorption of Poly(Hexamethylenebiguanide) on Cellulose: Mechanism of Binding and Molecular Recognition. *Langmuir* **2006**, *22* (13), 5636−5644.

(15) Tom, A. M.; Rajesh, R.; Vemparala, S. Aggregation Dynamics of Rigid Polyelectrolytes. *J. Chem. Phys.* **2016**, *144* (3), 034904.

(16) Vazdar, M.; Heyda, J.; Mason, P. E.; Tesei, G.; Allolio, C.; Lund, M.; Jungwirth, P. Arginine "Magic": Guanidinium Like-Charge Ion Pairing from Aqueous Salts to Cell Penetrating Peptides. *Acc. Chem. Res.* **2018**, *51* (6), 1455−1464.

(17) Nguyen, M. T. H.; Vazdar, M. Molecular Dynamics Simulations Unveil the Aggregation Patterns and Salting out of Polyarginines at Zwitterionic POPC Bilayers in Solutions of Various Ionic Strengths. *Comput. Struct. Biotec. J.* **2024**, *23*, 3897−3905.

(18) Sowlati-Hashjin, S.; Carbone, P.; Karttunen, M. Insights into the Polyhexamethylene Biguanide (PHMB) Mechanism of Action on Bacterial Membrane and DNA: A Molecular Dynamics Study. *J. Phys. Chem. B* **2020**, *124* (22), 4487−4497.

(19) Frisch, M. J.; Trucks, G. W.; Schlegel, H. B.; Scuseria, G. E.; Robb, M. A.; Cheeseman, J. R.; Scalmani, G.; Barone, V.; Petersson, G. A.; Nakatsuji, H., et al. *Gaussiañ16 Revision B.01*; Gaussian, Inc., 2016.

(20) Lu, T.; Chen, F. Multiwfn: A Multifunctional Wavefunction Analyzer. *J. Comput. Chem.* **2012**, *33* (5), 580−592.

(21) Humphrey, W.; Dalke, A.; Schulten, K. VMD: Visual molecular dynamics. *J. Mol. Graphics* **1996**, *14* (1), 33−38.

(22) Johnson, E. R.; Keinan, S.; Mori-Sánchez, P.; Contreras-García, J.; Cohen, A. J.; Yang, W. Revealing Noncovalent Interactions. *J. Am. Chem. Soc.* **2010**, *132* (18), 6498−6506.

(23) Lu, T.; Chen, Q. Independent Gradient Model Based on Hirshfeld Partition: A New Method for Visual Study of Interactions in Chemical Systems. *J. Comput. Chem.* **2022**, *43* (8), 539−555.

(24) Steiner, T. The Hydrogen Bond in the Solid State. *Angew. Chem., Int. Ed.* **2002**, *41* (1), 48−76.

(25) Emamian, S.; Lu, T.; Kruse, H.; Emamian, H. Exploring Nature and Predicting Strength of Hydrogen Bonds: A Correlation Analysis Between Atoms-in-Molecules Descriptors, Binding Energies, and Energy Components of Symmetry-Adapted Perturbation Theory. *J. Comput. Chem.* **2019**, *40* (32), 2868−2881.

(26) Geuenich, D.; Hess, K.; Köhler, F.; Herges, R. Anisotropy of the Induced Current Density (ACID), a General Method To Quantify and Visualize Electronic Delocalization. *Chem. Rev.* **2005**, *105* (10), 3758−3772.

(27) Mitoraj, M. P.; Michalak, A.; Ziegler, T. A Combined Charge and Energy Decomposition Scheme for Bond Analysis. *J. Chem. Theory Comput.* **2009**, *5* (4), 962−975.

(28) Abraham, M. J.; Murtola, T.; Schulz, R.; Páll, S.; Smith, J. C.; Hess, B.; Lindahl, E. GROMACS: High Performance Molecular Simulations through Multi-Level Parallelism from Laptops to Supercomputers. *SoftwareX* **2015**, *1*, 19−25.

(29) Wang, J.; Wolf, R. M.; Caldwell, J. W.; Kollman, P. A.; Case, D. A. Development and Testing of a General Amber Force Field. *J. Comput. Chem.* **2004**, *25* (9), 1157−1174.

(30) Lu, T. *Sobtop, Version [1.0(dev3.1)]*, 2022. http://sobereva.com/soft/Sobtop. (accessed on 2024 December 12).

(31) Lu, T.; Chen, Q. Simple, Efficient, and Universal Energy Decomposition Analysis Method Based on Dispersion-Corrected Density Functional Theory. *J. Phys. Chem. A* **2023**, *127* (33), 7023−7035.
(32) Miller, B. R.; McGee, T. D.; Swails, J. M.; Homeyer, N.; Gohlke, H.; Roitberg, A. E. MMPBSA.Py: An Efficient Program for End-State Free Energy Calculations. *J. Chem. Theory Comput.* **2012**, *8* (9), 3314−3321.
(33) Valdés-Tresanco, M. S.; Valdés-Tresanco, M. E.; Valiente, P. A.; Moreno, E. gmx_MMPBSA: A New Tool to Perform End-State Free Energy Calculations with GROMACS. *J. Chem. Theory Comput.* **2021**, *17* (10), 6281−6291.
(34) Marenich, A. V.; Cramer, C. J.; Truhlar, D. G. Universal Solvation Model Based on Solute Electron Density and on a Continuum Model of the Solvent Defined by the Bulk Dielectric Constant and Atomic Surface Tensions. *J. Phys. Chem. B* **2009**, *113* (18), 6378−6396.
(35) Ho, J.; Klamt, A.; Coote, M. L. Comment on the Correct Use of Continuum Solvent Models. *J. Phys. Chem. A* **2010**, *114* (51), 13442−13444.
(36) Israelachvili, J.; Pashley, R. The Hydrophobic Interaction Is Long Range, Decaying Exponentially with Distance. *Nature* **1982**, *300* (5890), 341−342.

https://doi.org/10.1021/acs.jpcc.4c07047
J. Phys. Chem. C 2025, 129, 2691−2700